Chapter 4

b) Adsorptive removal of Methylene blue using Zirconium tungstate

4b.1 Introduction

Tetravalent metal acid salts are amorphous and crystalline materials having general formula M(IV) $(HXO_4)_2.nH_20$, where M(IV)= Zr, Ti, Th, Ce, Sn, etc and X = P, Mo, W, Sb, As, etc. These substances are known as inorganic ion exchangers because they can exchange the protons of the OH group for a variety of metal ions (Academy & Chemislry, 1998). Therefore, many researchers had tried to develop tetravalent acid salts for adsorption application purpose. S.A. Nabi et al. synthesized pyridine anchored tin(IV) tungstoselenate for adsorption of various metal ions such as Cu^{2+}, Co^{2+}, Ni^{2+}, Fe^{2+}, Fe^{3+} (S A Nabi et al., 2000). Tarun Parangi et al. investigated cerium phosphate for the sorption of heavy metal ions like Co^{2+}, Ni^{2+}, Cu^{2+}, Zn^{2+}, Cd^{2+}, Hg^{2+}, and Pb^{2+} (Taylor et al., 2015). Titanum phosphate was also developed for the sorption of Mn^{+2}, Ni^{+2}, Cu^{+2}, Zn^{+2} (Maheria & Chudasama, 2007).

Zirconium Tungstate is a tetravalent metal acid salt that exhibits a negative coefficient of thermal expansion (CTE) over a wide temperature range (Mary et al., 1996). The tungstates are thermodynamically stable at high temperatures (CHANG et al., 1967). Zirconium tungstate-based materials have been used in a wide range of applications like microelectronics (CHANG et al., 1967)(Holzer & Dunand, 1999), low CTE polymer composites (Verma et al., 2008)(Zhao et al., 2013)(Lind et al., 2011), construction materials (Kofteros et al., 2001), substrates for mirrors and optical devices (Yang et al., 2008) and ZrW_2O_8 was also discovered to be a novel photocatalyst for hydrogen production from photocatalytic water splitting (Jiang et al., 2010). Syed Ashfaq Nabi et al. synthesized zirconium tungstate for the treatment of industrial waste water and synthetic mixtures of metal ions (Syed Ashfaq Nabi et al., 2012).

Several researchers have reported the use of zirconium based oxometallates for adsorption purpose**.** Natrayasamy Viswanathan and S. Meenakshi had investigated the adsorption of fluoride onto chitosan supported zirconium (IV) tungstophosphate composite (Jiang et al., 2010). Ahmed et al. used zirconium silico-tungstate matrix for adsorption of U (VI) from chloride solutions (Eliwa & Mubark, 2021). Gaurav S et al synthesized chitin-poly(itaconic acid-co-acrylamide)/zirconium tungstate nanocomposite hydrogel and used it for removal of fast sulphon black dye (Sharma et al., 2021). Vinisha and Janardan prepared Polyaniline embedded tin zirconium tungstate composite for the removal of heavy metal ion and organic pollutants from aqueous solution (Fecht, 2015). V. Ageetha et al. synthesized zirconium tungstate and its composite with chitosan by sol gel method (Vanamudan et al., 2018). The material was used for the catalytic degradation of single and binary mixture of dyes. In this study zirconium tungstate was prepared by sol gel method and calcined to be applied for the removal of methylene blue from waste water and effluents. Preliminary studies on fluoride removal revealed very low removal efficiency of 9.74 mg/g of adsorbent at pH 1 which is not quite feasible for drinking water purpose. So being a cation exchanger, ZrW was used for the removal of cationic dye such as methylene blue from the aqueous solutions.

4b.2 Material and methods

4b.2.1 Materials

Sodium tungstate (Na_2WO_4, Merck; 99.9%), Zirconium oxy chloride ($ZrOCl_2.8H_2O$, Spectrachem), Methylene blue ($C_{16}H_{18}N_3SCl.3H_2O$) (Sigma) was used in this study without further purification. The stock solution was prepared by dissolving required amount of dye in distilled water.

4b.2.2 Synthesis of Zirconium tungstate (ZrW)

Zirconium tungstate (ZrW) was synthesized by adding an aqueous solution of sodium tungstate to an aqueous solution of zirconium oxychloride in 2:1 molar proportion under stirring condition at room temperature. White precipitates of zirconium tungstate were formed which were stirred for 2 h for complete precipitation. Then it was then kept in autoclave for 1 h at 15 psi pressure. The precipitates were then centrifuged and washed several times with conductivity water and dried at 50°C. The obtained material was further calcined at 1100° C to form ZrW_2O_8.

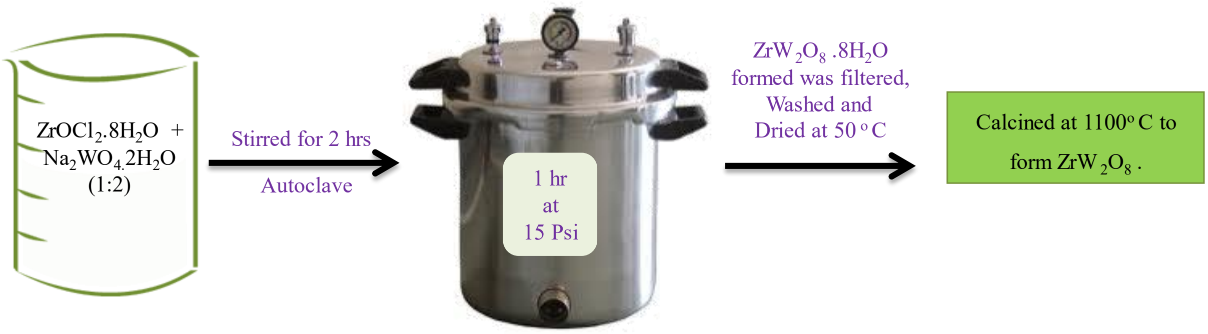

4b.2.3 Adsorption experiments

Stock solutions of 1000 mg/L was prepared by dissolving 1000 mg of MB dye in 1000 ml of conductivity water. The batch adsorption experiments were conducted for uptake studies. For experimental studies 25 mL of MB was agitated with 100 mg of adsorbent in a 150 mL conical flask for 2 h in an orbital shaker at 150 rpm. After adsorption the UV spectra of the supernatant was taken to determine the residual concentration from previously recorded calibration spectra. The amount of methylene blue uptake was calculated using the formula:

$$q_e = \frac{C_i - C_e}{m} \times 100$$

where q_e is the methylene blue uptake (mg/g), C_i is initial methylene blue concentration (mg/L), C_e is equilibrium methylene blue concentration (mg/L) and m is mass of the material (mg).

The factors affecting the MB uptake like pH, dose of ZrW, time, temperature and initial MB concentration were studied. Initial pH of the methylene blue solution was adjusted using 0.1 M NaOH and 0.1 M HCl. Other experiments were conducted at neutral pH.

4b.3 Results and discussion

4b.3.1 Characterization of ZrW

Morphology analysis (SEM- EDS)

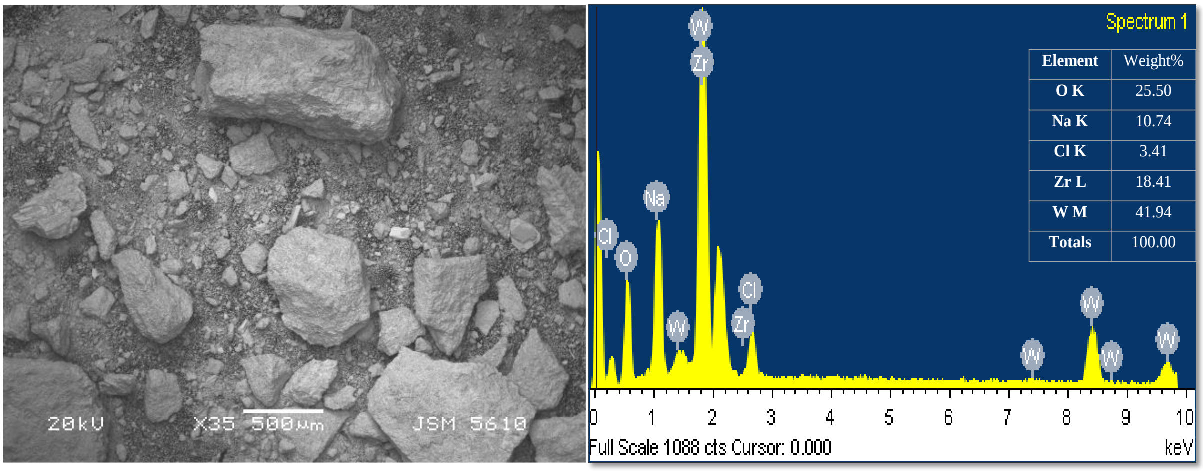

Figure 4b.1 SEM and EDS spectra of ZrW

ZrW show irregular morphology. The EDS spectrum shown in figure 4b.1 confirmed that zirconium and tungsten are main components present in ZrW (empirical formula $Na_3Zr_3W_5O_{22}Cl$).

FTIR spectroscopy

Figure 4b.2 shows the FTIR spectra of ZrW and ZrWMB. The broad intense peak in the region at 3394 cm^{-1} is attributed to the O–H stretching of lattice water molecules in ZrW. The intense sharp peaks at 1690 and 1623 cm^{-1} in ZrW and ZrWMB respectively may be attributed to H–O–H bending indicating the presence of interstitial water.

The bending vibration peaks of -W-O at 523 and 597 cm^{-1} has been shifted to 520 and 589 cm^{-1}in ZrWMB which indicates the interaction of ZrW with methylene blue molecules. The bands in the regions 828-769 and 925-828 cm^{-1} can be assigned to $(WO_4)^{2-}$ and W-O stretching vibrations, respectively (Badrinarayanan et al., 2011). The bands in the range 600-400 cm^{-1} can be attributed to WO_4 asymmetric bending modes and Zr-O stretching modes in ZrW and ZrWMB.

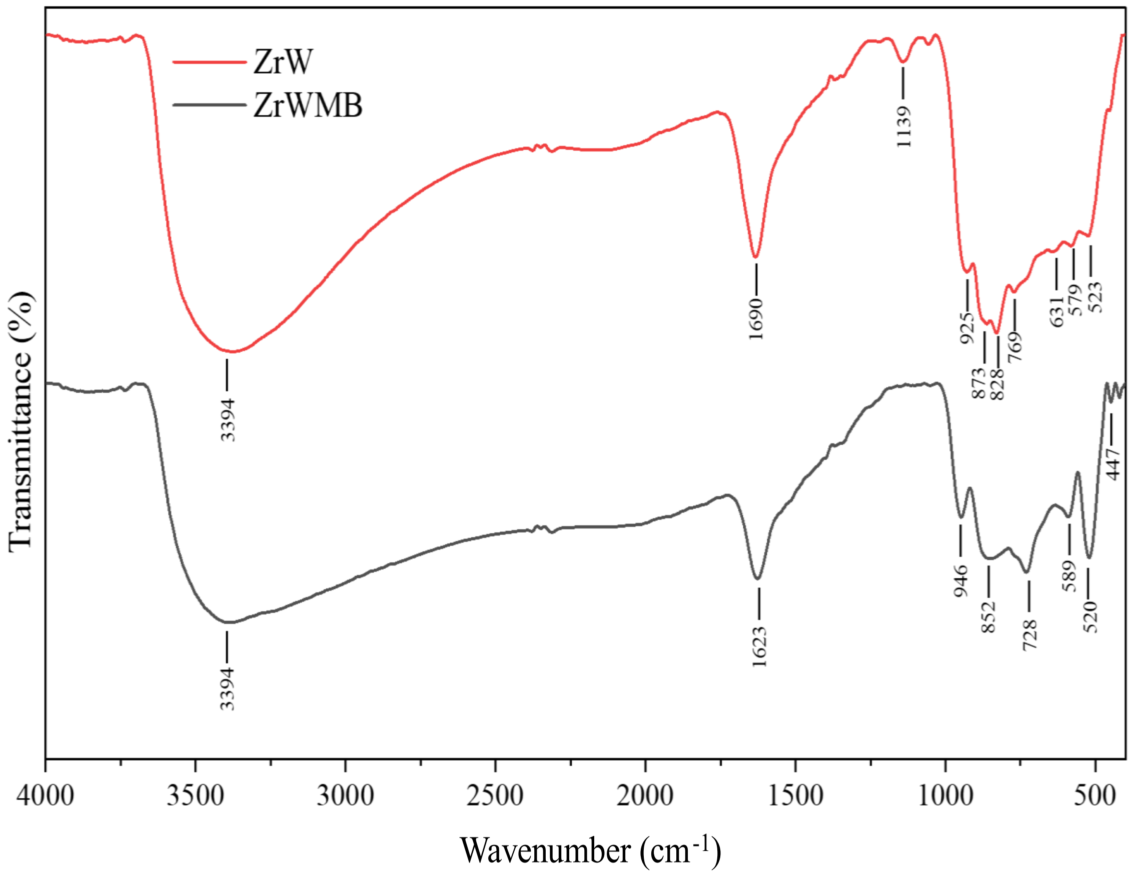

Figure 4b.2 Infrared spectra spectra of ZrW before and after adsorption of methylene blue (ZrWMB)

X-Ray diffraction analysis

The XRD pattern can be indexed to cubic ZrW_2O_8 and the spectra revealed increase in interlayer spacing after adsorption of methylene blue indicating probable electrostatic attraction with interlayer anions. The average crystallite size was observed to be 3.59 nm.

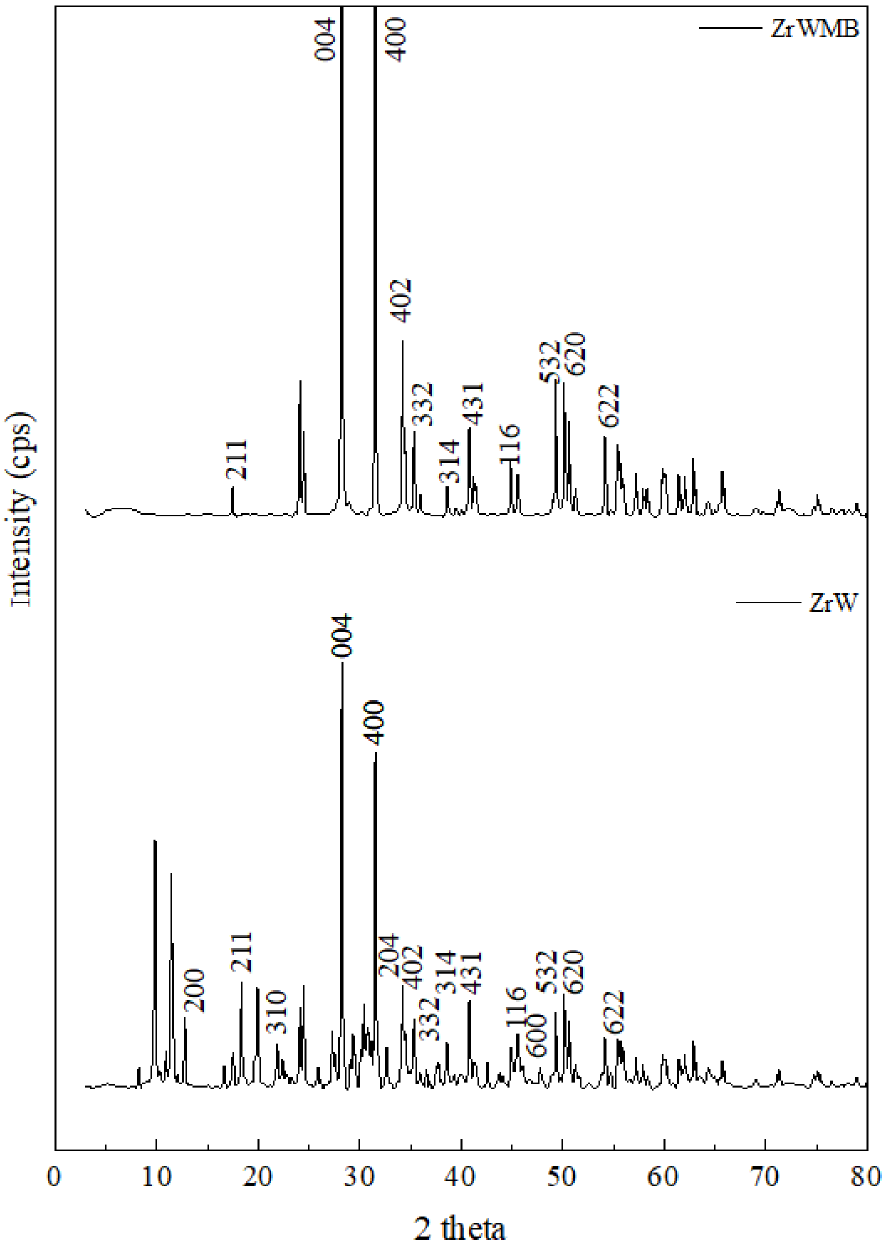

Figure 4b. 3 XRD Spectrum of ZrW before and after adsorption of methylene blue

Thermogravimetric analysis

Figure 4b.4 shows the thermal stability and degradation behavior of ZrW observed from TGA under nitrogen atmosphere. The total weight loss in ZrW was seen to be approximately 1.4%. About 0.3% loss in weight due to loss of adsorbed water occurred in the temperature range 50-110ºC for ZrW followed by a stable phase and another weight loss of 0.6% at 500-550ºC

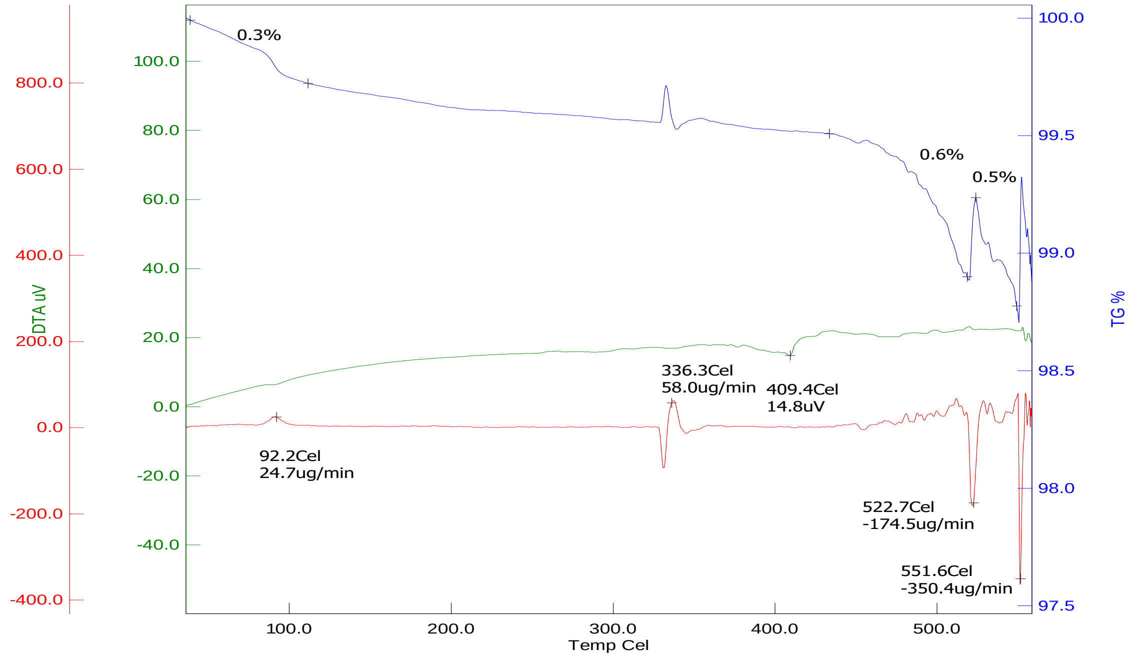

Figure 4b. 4 Thermogravimetry analysis of ZrW

DSC analysis

The DSC spectra of ZrW is shown in figure 4b.5. The endothermic peaks upto 200°C indicate loss of water and phase transition from α- ZrW_3O_8 to β-ZrW_2O_8 while the endothermic peak at 330°C as a transition to formation of new structures.

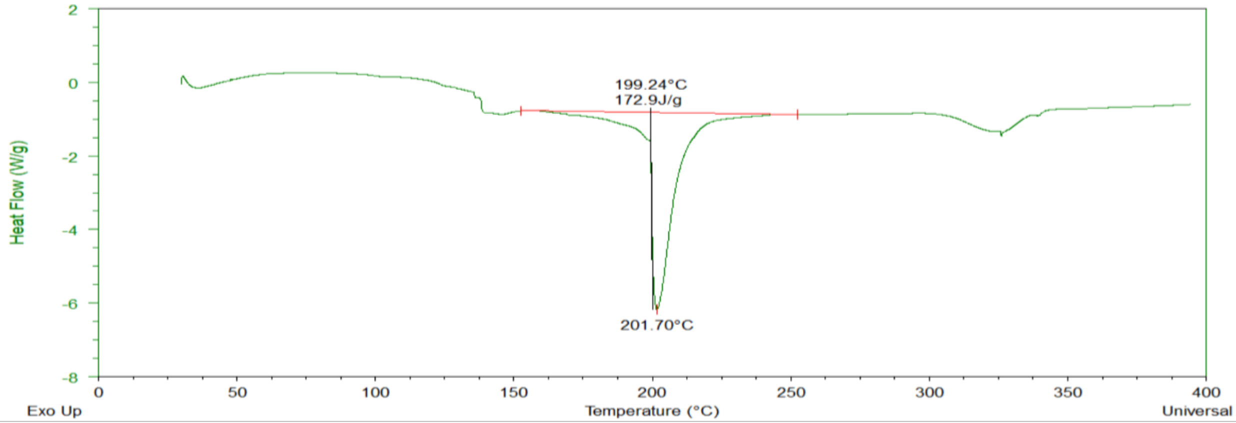

Figure 4b. 5 DSC spectra of ZrW

4b.3.2 Effect of pH

The pH of a dye solution is an important influencing factor for the adsorption MB onto ZrW. Figure 4a.6 shows the effect of pH on adsorption of MB onto ZrW. The study was done at pH range 1.0–11.0 using 25 mL of 100 mg/L MB solution and agitating for 2 h. There was no significant effect of pH observed on percentage uptake of fluoride, so further studies were carried out at neutral pH.

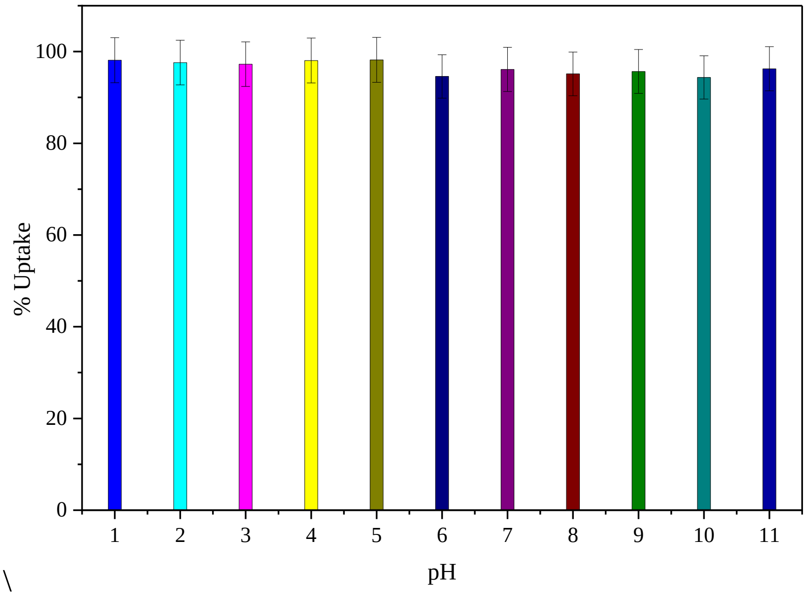

\

Figure 4b. 6 Effect of pH on % uptake of methylene blue (contact time: 2 h, dose: 100 mg, C_i: 100 mg/L)

4b.3.3 Effect of dose

The adsorbent doses were varied from 25 mg to 300 mg/25 mL. It was evident from figure 4b.7 that the MB removal increased with increase in the adsorbent dose due to availability of more adsorbent sites as well as greater availability of specific surface area of ZrW. However, no significant changes in removal efficiency were observed beyond 100 mg/100 mL adsorbent dose. Due to agglomeration of adsorbent particles, there is no increase in adsorption efficiency beyond 100 mg/100 mL ZrW. So, 100 mg/25 ml was considered the optimal dose for adsorption.

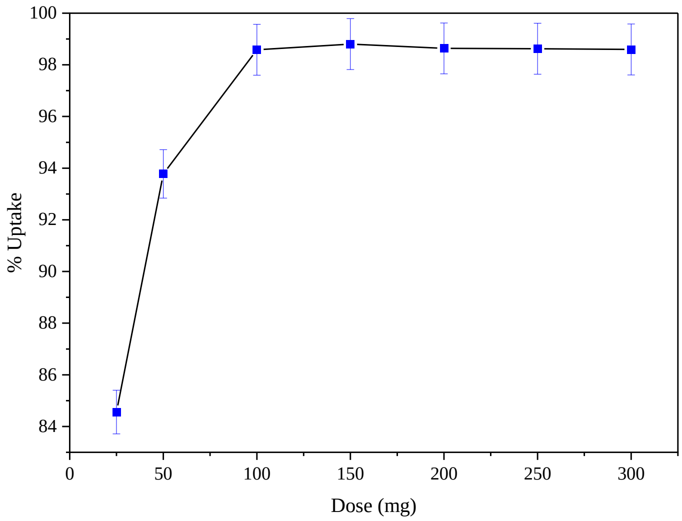

Figure 4b. 7 Effect of dose on % uptake of methylene blue (contact time: 2 h, conc.: 100 mg/L)

4b.3.4 Effect of initial MB concentration

The effect of MB concentration on adsorption capacity of ZrW was studied in the concentration range of 50–1000 mg/L (figure 4b.8). Increase in dye concentration showed no significant changes in removal efficiency because with increased MB concentration the driving force for mass transfer also increased. At low concentration, there would be unoccupied active sites on the adsorbent surface.

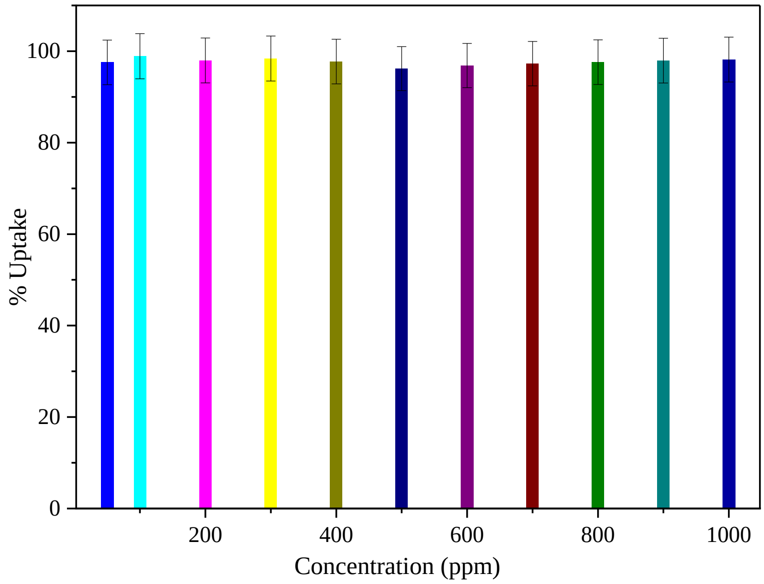

Figure 4b. 8 Effect of initial MB concentration on % uptake of methylene blue (dose: 100 mg, contact time: 2 h)

4b.3.5 Effect of temperature

Adsorption of MB by ZrW was not affected in temperature range 303 to 333 K (Figure 4b.9).

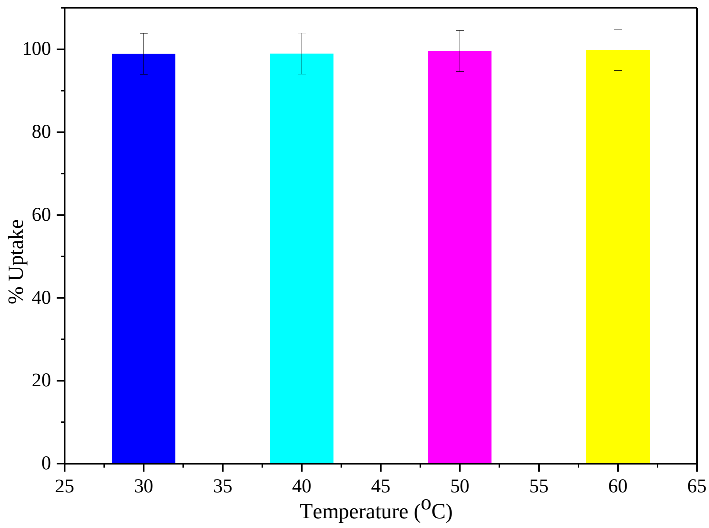

Figure 4b. 9 Effect of temperature on % uptake of MB (dose: 100 mg, conc.: 100 mg/L, contact time: 2 h

4b.3.6 Effect of contact time

The effect of contact time on MB uptake is shown in Figure 4b.10. In 120 min, 98 % of dye removal was observed. The equilibrium was reached after 120 min. This change in rate of adsorption may be due to fact that initially all the adsorbent sites are vacant and solute concentration gradient is very high. After equilibrium, the decrease in the rate of adsorption may be due to decrease in number of vacant sites of adsorbent and dye concentration.

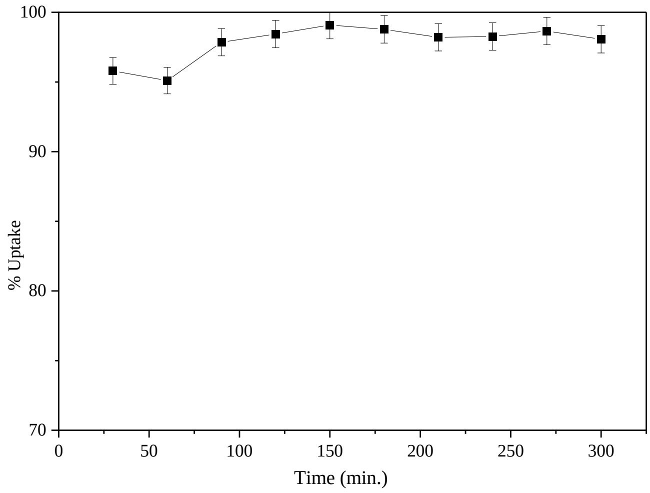

Figure 4b.10 Effect of contact time on % uptake of MB (dose: 100 mg, conc.: 100 mg/L)

4b.3.7 Adsorption isotherm

The adsorption capacity and other isotherm parameters were evaluated using Langmuir and Freundlich, Temkin and Halsey isotherm models. The isotherm plots of Halsey and Temking have not been shown . The parametric constants have been tabulated in table 4b.1. It has been observed that the sorption capacity (q_m) was found to be 239.85 mg/g (table 4b.1). The low correlation value for Temkin isotherm indicated that the adsorption process did not depend on the heat of adsorption as also observed by temperature studies. The equilibrium data were fitted to Freundlich equation. The parameters n and K_F indicated the sorption intensity and the sorption capacity of the system. The magnitude of the term (1/n) gives an indication of the favourability of the sorbent/adsorbate systems (Malik, 2004). The correlation coefficient value (0.99) was higher than Langmuir model values. The fitting of Halsey model also exhibited reasonably good correlation value of 0.95. Therefore, adsorption onto ZrW fitted Freundlich isotherm i.e multilayer adsorption onto a heterogeneous surface.. The comparision of maximum adsorption capacity of ZrW with literature reported adsorbents are summarised in table 4b.4. ZrW exhibited beter adsorption characteristics as compared to other literature reported Zr based adsorbents with a high adsorption capacity over a wide pH range.

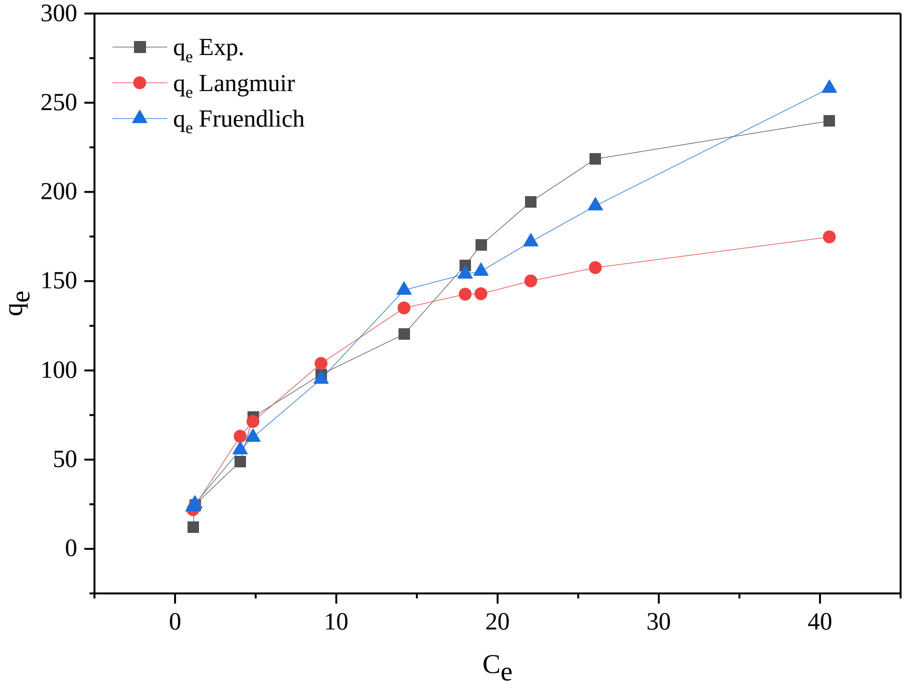

Figure 4b. 11 Adsorption isotherms

Table 4b.1 Various isotherm plots for the adsorption of MB onto ZrW

	Isotherm Parameters		
Langmuir	Q_m	K_L (L.mmol^{-1})	r^2
	217.39	0.1011	0.89
Freundlich	N	k_F(L.g^{-1})	r^2
	1.19	21.92	0.99
Temkin	A_T (Lg^{-1})	b_T	r^2
	0.1705	0.0065	0.88
Halsey	k_H (L.g^{-1})	n_H	r^2
	42.06	1.322	0.95

Table 4b. 2 Comparison with other reported adsorbents

Adsorbent	pH	Q_{max}	Ref.
Polyaniline zirconium (IV) silicophosphate nanocomposite	1.0	12	(Vinod Kumar Gupta et al., 2014)
Micro-Mesoporous Zr_3O/Activated Carbon Composite	7.5	208.33	(Ait Ahsaine et al., 2018)
guar gum–cerium (IV) tungstate hybrid cationic exchanger	9.0	120.68	(V K Gupta et al., 2014)
Zirconium Phosphate-Coated Polyaniline Composite	2.0-11.0	120.48	(Obulapuram et al., 2021)
ZrO_2/Polyaniline nanocomposite	7.0	10.4	(Kumar et al., 2020)
Sulphated zirconium supported MCM-41 composite	10.0	186	(Ibrahim et al., 2021)
alumina–zirconia composite	9.0	53.44	(Adesina et al., 2019)
ZrW	1.0-10.0	239.85	This study

4b.3.8 Adsorption kinetics

The data for the adsorption of MB on ZrW was applied to pseudo-first- and second-order kinetic models and the results are presented in Table 4b.3. The correlation coefficient of second-order kinetic model (0.99) was greater than for first-order kinetic model (0.84) (figure 4b.12). This affirmed that the rate limiting step was chemisorption, involving valence forces through sharing or exchange of electron.

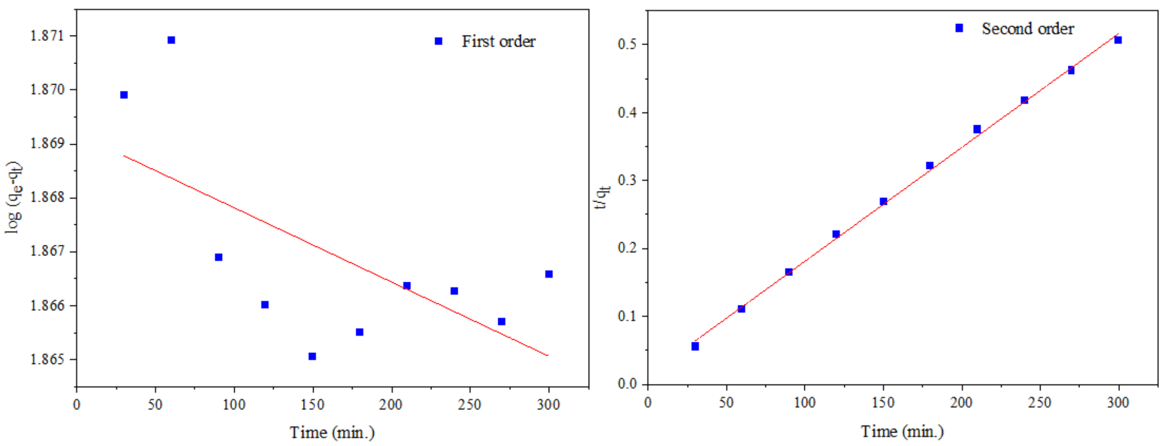

Figure 4b. 12 Kinetic models

Table 4b. 3 Kinetic parameters

q_{exp}: 25.51	**q_t**	**K**	**r^2**
Pseudo First order	74.07	$6.9*10^{-5}$	0.84
Pseudo Second order	24.75	0.0486	0.99

4b.3.9 Reuse of adsorbent

To study the reusability of adsorbent, adsorption-desorption phenomenon had been applied. For this desorption was performed (using 0.1 M NaOH) followed by drying of adsorbent. Then the adsorbent was reused again. The % uptake of MB was found to be 99.82%, 98.35%, 96.44% and 95.18% for 4 cycles respectively

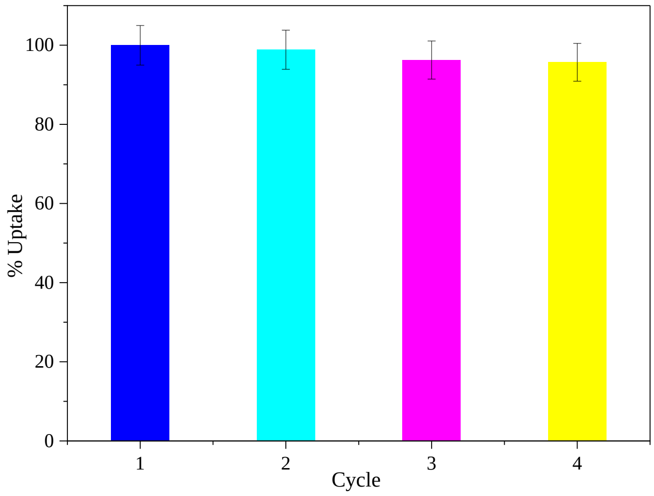

Figure 4b. 13 % uptake of methylene blue after consecutive 1^{st} 2^{nd} 3^{rd} and 4^{th} cycles

4b.4 Conclusion

The tetravalent metal acid salt, zirconium tungstate was successfully synthesized by sol-gel method. The synthesized zirconium tungstate was observed to have irregular morphology. The XRD spectra revealed the presence of cubic form of zirconium tungstate with average crystallite size of 3.59 nm. It was used for the treatment of synthetic dye effluent as well as for the adsorption of methylene blue from the aqueous solutions with maximum adsorptions capacity of 239.85 mg/g. The material can also be used for various cationic dyes further.

4b.5 References

Academy, I., & Chemislry, A. (1998). *Synthesis , characterization and application of a derivatized acid salt of tetravalent metal : o-chlorophenol anchored onto zirconium tungstate*. *21*(3), 189–193.

Adesina, A., Elvis, O., Mohallem, N., & J. Olusegun, S. (2019). Adsorption of Methylene blue and Congo red from aqueous solution using synthesized alumina–zirconia composite. *Environmental Technology*, *42*, 1–10. https://doi.org/10.1080/09593330.2019.1652696

Ait Ahsaine, H., Anfar, Z., Zbair, M., Ezahri, M., & Alem, N. (2018). Adsorptive Removal of Methylene Blue and Crystal Violet onto Micro-Mesoporous Zr_3O/Activated Carbon Composite: A Joint Experimental and Statistical Modeling Considerations. *Journal of Chemistry*, *2018*, 1-15. https://doi.org/10.1155/2018/6982014

Badrinarayanan, P., Ahmad, M. I., Akinc, M., & Kessler, M. R. (2011). Synthesis, processing, and characterization of negative thermal expansion zirconium tungstate nanoparticles with different morphologies. *Materials Chemistry and Physics*, *131*(1–2), 12–17. https://doi.org/http://dx.doi.org/10.1016/j.matchemphys.2011.09.055

CHANG, L. L. Y., SCROGER, M. G., & PHILLIPS, B. (1967). Condensed Phase Relations in the Systems ZrO2-WO2-WO3 and HfO2-WO2-WO3. *Journal of the American Ceramic Society*, *50*(4), 211–215. https://doi.org/https://doi.org/10.1111/j.1151-2916.1967.tb15084.x

Eliwa, A. A., & Mubark, A. E. (2021). Effective sorption of U(VI) from chloride solutions using zirconium silico-tungstate matrix. *International Journal of Environmental Analytical Chemistry*, 1–19. https://doi.org/10.1080/03067319.2021.1921762

Fecht, H. J. (2015). Materials science. *Generation and Applications of Extra-Terrestrial Environments on Earth*, *13*(9), 211–220. https://doi.org/10.1177/0022034585064005120

Gupta, V K, Pathania, D., Singh, P., Kumar, A., & Rathore, B. S. (2014). Adsorptional removal of methylene blue by guar gum–cerium (IV) tungstate hybrid cationic exchanger. *Carbohydrate Polymers*, *101*, 684–691. https://doi.org/https://doi.org/10.1016/j.carbpol.2013.09.092

Gupta, Vinod Kumar, Pathania, D., Kothiyal, N. C., & Sharma, G. (2014). Polyaniline zirconium (IV) silicophosphate nanocomposite for remediation of methylene blue dye from waste water. *Journal of Molecular Liquids*, *190*, 139–145. https://doi.org/10.1016/j.molliq.2013.10.027

Holzer, H., & Dunand, D. C. (1999). Phase transformation and thermal expansion of Cu/ZrW2O8 metal matrix composites. *Journal of Materials Research*, *14*(3), 780–789. https://doi.org/DOI: 10.1557/JMR.1999.0104

Ibrahim, A. A., Salama, R. S., El-Hakam, S. A., Khder, A. S., & Ahmed, A. I. (2021). Synthesis of sulfated zirconium supported MCM-41 composite with high-rate adsorption of methylene blue and excellent heterogeneous catalyst. *Colloids and Surfaces A: Physicochemical and Engineering Aspects*, *616*, 126361. https://doi.org/https://doi.org/10.1016/j.colsurfa.2021.126361

Jiang, L., Wang, Q., Li, C., Yuan, J., & Shangguan, W. (2010). ZrW_2O_8 photocatalyst and its visible-light sensitization via sulfur anion doping for water splitting. *International Journal of Hydrogen Energy*, *35*(13), 7043–7050. https://doi.org/https://doi.org/10.1016/j.ijhydene.2009.12.187

Kofteros, M., Rodriguez, S., Tandon, V., & Murr, L. E. (2001). A preliminary study of thermal expansion compensation in cement by ZrW_2O_8 additions. *Scripta Materialia*, *45*(4), 369–374. https://doi.org/10.1016/S1359-6462(01)01009-0

Kumar, N., Bahl, T., & Kumar, R. (2020). Study of the methylene blue adsorption mechanism using ZrO_2/Polyaniline nanocomposite. *Nano Express*, *1*(3), 30025. https://doi.org/10.1088/2632-959x/abca10

Lind, C., Coleman, M. R., Kozy, L. C., & Sharma, G. R. (2011). Zirconium tungstate/polymer nanocomposites: Challenges and opportunities. *Physica Status Solidi (B)*, *248*(1), 123–129. https://doi.org/https://doi.org/10.1002/pssb.201083967

Maheria, K., & Chudasama, U. (2007). *Kinetics , thermodynamics and sorption characteristics of an inorganic ion exchanger , titanium phosphate , towards first row transition metal ions*. *46*(March), 449–454.

Malik, P. K. (2004). Dye removal from wastewater using activated carbon developed from sawdust: Adsorption equilibrium and kinetics. *Journal of Hazardous Materials*, *113*(1–

3), 81–88. https://doi.org/10.1016/j.jhazmat.2004.05.022

Mary, T. A., Evans, J. S. O., Vogt, T., Sleight, A. W., Barron, T., Bienenstock, A., Blackman, M., Brown, I. D., Chang, L., Evans, J., Gale, J. D., Graham, J., Hazen, R. M., Korthuis, V., Martinek, C., Mary, T. A., Roy, R., Sleight, A. W., Trunov, V. K., & White, G. K. (1996). Negative Thermal Expansion from 0.3 to 1050 Kelvin in ZrW_2O_8. *Science*, *272*(5258), 90–92. https://doi.org/10.1126/science.272.5258.90

Nabi, S A, Islam, A., & Rahman, N. (2000). *Synthesis , Characterization and Application of a Derivatized Acidic Salt of a Tetravalent Metal . Pyridine Anchored on to Tin (IV) Tungstoselenate*. *Iv*, 551–560. https://doi.org/10.1260/0263617001493611

Nabi, Syed Ashfaq, Bushra, R., & Shahadat, M. (2012). Application of Zr(IV) tungstate for removal of metal ions from aqueous solutions. *Toxicological and Environmental Chemistry*, *94*(3), 468–481. https://doi.org/10.1080/02772248.2011.651084

Obulapuram, P. K., Arfin, T., Mohammad, F., Kumari, K., Khiste, S. K., Al-Lohedan, H. A., & Chavali, M. (2021). Surface-Enhanced Biocompatibility and Adsorption Capacity of a Zirconium Phosphate-Coated Polyaniline Composite. *ACS Omega*, *6*(49), 33614–33626. https://doi.org/10.1021/acsomega.1c04490

Sharma, G., Kumar, A., Naushad, M., Thakur, B., Vo, D.-V. N., Gao, B., Al-Kahtani, A. A., & Stadler, F. J. (2021). Adsorptional-photocatalytic removal of fast sulphon black dye by using chitin-cl-poly(itaconic acid-co-acrylamide)/zirconium tungstate nanocomposite hydrogel. *Journal of Hazardous Materials*, *416*, 125714. https://doi.org/https://doi.org/10.1016/j.jhazmat.2021.125714

Taylor, P., Parangi, T., Wani, B., & Chudasama, U. (2015). *Desalination and Water Treatment Sorption and separation study of heavy metal ions using cerium phosphate : a cation exchanger*. *April*, 37–41. https://doi.org/10.1080/19443994.2015.1008582

Thue, P. S., Sophia, A. C., Lima, E. C., Wamba, A. G. N., de Alencar, W. S., dos Reis, G. S., Rodembusch, F. S., & Dias, S. L. P. (2018). Synthesis and characterization of a novel organic-inorganic hybrid clay adsorbent for the removal of acid red 1 and acid green 25 from aqueous solutions. *Journal of Cleaner Production*, *171*, 30–44. https://doi.org/10.1016/j.jclepro.2017.09.278

Vanamudan, A., Sadhu, M., & Pamidimukkala, P. S. (2018). Nanostructured zirconium tungstate and its bionanocomposite with chitosan: Wet peroxide photocatalytic degradation of dyes. *Journal of the Taiwan Institute of Chemical Engineers*, *85*, 74–82. https://doi.org/10.1016/j.jtice.2017.12.018

Verma, A. S., Kumar, A., & Bhardwaj, S. R. (2008). Correlation between ionic charge and the lattice constant of cubic perovskite solids. *Physica Status Solidi (B)*, *245*(8), 1520–1526. https://doi.org/https://doi.org/10.1002/pssb.200844072

Yang, X., Cheng, X., Li, H., Xu, J., & Sun, X. (2008). Thermal and electric conductivity of near-zero thermal expansion ZrW_2O_8/ZrO_2 composites. *Journal of the Ceramic Society of Japan*, *116*(3), 471–474.

Zhao, C., Wang, C., Yue, Z., Shu, K., & Wallace, G. G. (2013). Intrinsically Stretchable Supercapacitors Composed of Polypyrrole Electrodes and Highly Stretchable Gel Electrolyte. *ACS Applied Materials & Interfaces*, *5*(18), 9008–9014. https://doi.org/10.1021/am402130j